AD-A168 894 THE EFFECT OF HIGH PRESSURE ON ELECTRICAL RELAXATION IN PPO AND ELECTRICA..(U) NAVAL ACADEMY ANNAPOLIS MD DEPT OF PHYSICS J J FONTANELLA ET AL. JUN 86 TR-22 1/1

UNCLASSIFIED F/G 7/4 NL

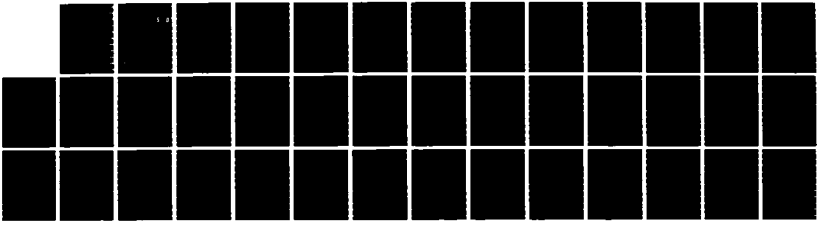

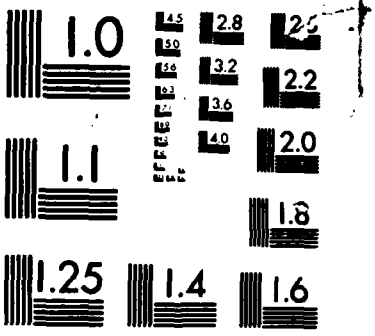
1.0
1.1
1.25
1.4
1.6
1.8
2.0
2.2
2.8
3.2
3.6
4.0
4.5
5.0
5.6

(16)

OFFICE OF NAVAL RESEARCH

Contract N00014-86-AF-00001

Task No. NR 627-793

TECHNICAL REPORT NO. 22

The Effect of High Pressure on Electrical Relaxation in PPO and Electrical Conductivity in PPO Complexed with Lithium Salts

by

John J. Fontanella & Mary C. Wintersgill

Prepared for Publication

in

Journal of Applied Physics, October 1986

U. S. Naval Academy
Department of Physics
Annapolis, MD 21402

June 1986

SECURITY CLASSIFICATION OF THIS PAGE (When Data Entered)

REPORT DOCUMENTATION PAGE		READ INSTRUCTIONS BEFORE COMPLETING FORM
1. REPORT NUMBER: 22	2. GOVT ACCESSION NO.	3. RECIPIENT'S CATALOG NUMBER
4. TITLE (and Subtitle): THE EFFECT OF HIGH PRESSURE ON ELECTRICAL RELAXATION IN PPO AND ELECTRICAL CONDUCTIVITY IN PPO COMPLEXED WITH LITHIUM SALTS		5. TYPE OF REPORT & PERIOD COVERED: Interim technical report 6. PERFORMING ORG. REPORT NUMBER
7. AUTHOR(s): JOHN J. FONTANELLA & MARY C. WINTERSGILL		8. CONTRACT OR GRANT NUMBER(s): N00014-86-AF-00001
9. PERFORMING ORGANIZATION NAME AND ADDRESS: Physics Department, U. S. Naval Academy, Annapolis, MD 21402		10. PROGRAM ELEMENT, PROJECT, TASK AREA & WORK UNIT NUMBERS: NR No. 627-793
11. CONTROLLING OFFICE NAME AND ADDRESS: Office of Naval Research, Attn. Code 413, 800 N. Quincy St., Arlington, VA 22217		12. REPORT DATE: June 1986 13. NUMBER OF PAGES: 15
14. MONITORING AGENCY NAME & ADDRESS(if different from Controlling Office)		15. SECURITY CLASS. (of this report) 15a. DECLASSIFICATION/DOWNGRADING SCHEDULE

16. DISTRIBUTION STATEMENT (of this Report)

Approved for public release and sale.
Distribution unlimited.

17. DISTRIBUTION STATEMENT (of the abstract entered in Block 20, if different from Report)

18. SUPPLEMENTARY NOTES

19. KEY WORDS (Continue on reverse side if necessary and identify by block number)

Solid electrolytes, polymer electrolytes, poly(propylene oxide), electrical relaxation, glass transition, electrical conductivity, high pressure, activation volume, activation energy.

20. ABSTRACT (Continue on reverse side if necessary and identify by block number)

Audio frequency electrical conductivity and relaxation studies have been carried out on Parel 58 elastomer and Parel 58 elastomer complexed with a variety of lithium salts. The measurements have been carried out in vacuum over the temperature range 5-380 K and at pressures up to 0.65 GPa over the temperature range 230-380 K. Both the electrical conductivity for the complexed material and the electrical relaxation time associated with the α relaxation in the uncomplexed material exhibit VTF or WLF behavior. From the VTF analysis for both the vacuum electrical relaxation time and

DD FORM 1 JAN 73 1473 EDITION OF 1 NOV 65 IS OBSOLETE
S/N 0102-014-6601 |

SECURITY CLASSIFICATION OF THIS PAGE (When Data Entered)

electrical conductivity, E_a is found to be about 0.09 eV and T_o is found to be about 40°C below the central glass transition temperature. In addition, it is found that the activation volumes for the electrical relaxation time and the electrical conductivity are the same when compared relative to T_o. These results imply that the mechanism controlling ionic conductivity is the same as that for the α relaxation namely large scale segmental motions of the polymer chain.

THE EFFECT OF HIGH PRESSURE ON ELECTRICAL RELAXATION IN PPO AND ELECTRICAL CONDUCTIVITY IN PPO COMPLEXED WITH LITHIUM SALTS*

J. J. Fontanella, M. C. Wintersgill, M. K. Smith, J. Semancik

Physics Department

U. S. Naval Academy

Annapolis, MD 21402

C. G. Andeen

Physics Department

Case Western Reserve University

Cleveland, OH 44106

ABSTRACT

Audio frequency electrical conductivity and relaxation studies have been carried out on Parel 58 elastomer and Parel 58 elastomer complexed with a variety of lithium salts. The measurements have been carried out in vacuum over the temperature range 5-380K and at pressures up to 0.65 GPa over the temperature range 230-380K. Both the electrical conductivity for the complexed material and the electrical relaxation time associated with the α relaxation in the uncomplexed material exhibit VTF or WLF behavior. From a VTF analysis for both the vacuum electrical relaxation time and electrical conductivity, E_a is found to be about 0.09 eV and T_o is found to be about 40^oC below the "central" glass transition temperature. In addition, it is found that the activation volumes for the electrical relaxation time and the electrical conductivity are the same when compared relative to T_o. These results imply that the mechanism controlling ionic conductivity is the same as that for the α relaxation namely large scale segmental motions of the polymer chain.

I. INTRODUCTION

A review of the work on ion conducting polymers has been given by Armand.[1] Subsequently, there has been a considerable amount of work in the field including many new ion conducting materials and new types of measurements.[2-13] To date, the material which has been studied most intensively, of course, is poly(ethylene oxide) (PEO). However, that material is highly crystalline which complicates the situation since it is generally believed that electrical transport in these materials takes place primarily in the amorphous region. Consequently, it is necessary to understand the relation between the crystalline and amorphous regions before definitive conclusions can be drawn concerning electrical transport in these materials. As an alternative approach, studies of poly(propylene oxide) (PPO) can be undertaken as it is possible to prepare highly amorphous ion containing material. Relatively little work has been carried out on that material.[14-17] In the present work, the effect of high pressure on the electrical properties has been studied. A preliminary report has been given elsewhere.[18] In the present paper, new measurements are reported and it is shown that the effect of high pressure on the electrical conductivity is very similar to the effect of high pressure on the alpha relaxation in the host material which provides strong evidence that, for PPO, ion transport is controlled by large-scale segmental motions characteristic of the glass-rubber transition.

II. EXPERIMENTAL

Audio frequency complex impedance/electrical relaxation measurements have been carried out using a fully automated spectrometer. The key element in the measurements is a CGA-82 microprocessor-controlled bridge operating at seventeen frequencies from 10-10^5 Hz. Vacuum measurements were carried out in a Precision Cryogenics CT-14 dewar controlled by a Lake Shore Cryotronics DRC-82 temperature controller using a silicon diode sensor. The high pressure measurements were carried out in a pressure vessel using either Spinesstic 22 (Exxon) or Fluorinert (3M Co.) FC-77 electronic liquid as the high pressure fluid. Differential scanning calorimetry measurements (DSC) were carried out using a DuPont 990 DSC. All systems were controlled using Apple II computers.

The material studied was Parel 58 (Hercules, Inc.) elastomer which is a sulfur-vulcanizable copolymer of propylene oxide and allyl glycidyl ether. As the primary constituent is propylene oxide, the material will be referred to throughout this paper as PPO. Samples were obtained by solution casting using methanol as the solvent. The salts, LiI, $LiCF_3SO_3$, $LiClO_4$, and LiSCN, were dried in a vacuum oven at approximately 110°C. All procedures including loading of the samples into the various sample holders were carried out in a dry box. FTIR measurements were carried out on both the salts and all polymers. It was found that all materials were dry except those containing LiSCN. Consequently, the results for those materials are included only for comparison and the results are not considered as reliable as those for the other three salts.

Aluminum electrodes were vacuum evaporated onto the surfaces of the material in either a three-terminal or two-terminal configuration. The

samples were about 1 mm thick and the electrodes about 4 mm in diameter.

III. RESULTS

A. Differential Scanning Calorimetry

The DSC results for PPO_8:LiI are shown in Fig. 1. The DSC results for the other materials are shown elsewhere.[18] It is clear that the materials are highly amorphous as they exhibit only a glass transition. For PPO_8:LiI, for example, the as-prepared PPO_8:LiI showed a complex glass transition beginning at about 268K and ending at about 298K. After quench, the glass transition sharpened with an onset of about 278K and completion at about 288K. The effect is attributed to the inhomogeneities in the materials. However, the "central" glass transition temperature was about the same, 283K, both before and after quench. The results for all materials are listed in Table I.

B. Electrical Conductivity

A typical complex impedance plot is shown in Fig. 1 of Ref. 18 or Fig. 2 of Ref. 13. A single depressed arc was usually observed over the frequency range of measurement. The data were analyzed using a Cole-Cole distribution:[1]

$$Z^* = \frac{Z_o}{1 + (i\omega\tau_o)^{(1-\alpha)}} \qquad (1)$$

where Z_o, τ_o, and α are the fitting parameters. As temperature increases, less of a semicircle is observed together with more slanted vertical line at lower frequencies representing blocking electrode effects.

In most cases, a best-fit of Eq. (1) to the data was obtained allowing values for the bulk resistance of the materials to be determined. For the remaining plots, a combination of the depressed arc and slanted vertical line was used to determine the bulk resistance.

Occasionally, such simple plots were not obtained, an extra circle being observed. In fact, this anomalous behavior was usually observed after the aluminum electrodes had been on the samples for several months and thus the extra peak was attributed to a chemical reaction between the electrodes and the material and was eliminated in the data analysis.

The conductance values, G, were then used, in conjunction with room temperature geometrical measurements, to calculate the electrical conductivity from:

$$\sigma = Gt/S \qquad (2)$$

where t is the thickness and S is the surface area. Neither compressibility nor thermal expansion effects are included in the data analysis.

The results of typical isobaric (data taken at a constant pressure after temperature has been varied) data runs are shown in Fig. 2. The curvature often observed for amorphous polymer systems is apparent. Consequently, the conductivity data were first analyzed via the VTF equation:[19]

$$\sigma = AT^{-1/2} \exp^{-[E_a/k(T-T_o)]} \qquad (3)$$

with the adjustable parameters A, E_a, and T_o. A non-linear least squares fit of Eq. (3) to the data was carried out and Table II contains the best-fit parameters.

Next, isothermal data (data taken a constant temperature after varying pressure) were also taken and typical results are shown in Fig. 3. The following equation:

$$\log_{10}\sigma = \log_{10}\sigma_o + aP + bP^2 \qquad (4)$$

was best fit to the isothermal data and the best-fit parameters are listed in Table III.

In order to check the results of the isobaric data runs, 0.1 and 0.2 GPa conductivities were calculated from the isothermal results using the vacuum results as a reference. The resultant best fit VTF parameters are also listed in Table II. It is seen that there is good agreement between the two approaches.

It is noted that the vacuum values for T_o are between 34 and 46°C lower than the "central" T_g's which were determined by DSC. Some of these results have been reported previously[18] and a similar result has also been recently reported for poly(dimethyl siloxane-ethylene oxide) co-polymer containing a sodium salt.[13] In the earlier paper,[18] it was stated that T_g was 30-40°C above T_o. However, in that paper T_g was defined as the "onset" T_g. A similar result is obtained in the present work since as is apparent from a comparison of the results in Tables I and II, the "onset" T_g is 23-28°C above T_o.

Such results are not unexpected since T_g-T_o is often on the order of

50°C for polymer systems.[20,21] Further, this phenomenon is consistent with the configurational entropy model[22,23] where T_o is interpreted as the temperature of zero configurational entropy which would be expected to occur at a much lower temperature than DSC T_g's. However, this result disagrees with those of other workers[12] for similar materials. Possible reasons for the discrepancy along with details of the data analysis technique used in the present work are given elsewhere.[13]

The first result of the high pressure work is that the previous result[18] that T_o for PPO_8:$LiCF_3SO_3$ increases about 10K/kbar is confirmed. This is to be compared to dT_g/dP=17K/kbar which was observed for the α relaxation in uncomplexed PPO.[18] That value is larger, but since T_o increases several K/kbar, it adds evidence that T_o is somehow related to the glass transition since this variation is typical of glass transitions. However, it is apparent from Table II that for PPO_8:$LiClO_4$ and PPO_8:LiI, T_o does not change much with increasing pressure. A relation between T_o and T_g will still be preserved, of course, if T_g does not increase much with pressure for these materials. This is not unreasonable since it is clear that T_g is strongly shifted by the salts for these materials. Consequently, it is found that for materials for which the vacuum T_g or T_o is shifted strongly by the salts, T_o does not shift much with pressure. High pressure DSC studies are currently underway to check this result.

Since it is often suggested that electrical conductivity in these materials is "liquid-like" it is of interest to compare the present results with the effect of high pressure on ionic conductivity in liquids. In particular, Angell et al.[24] have shown that while VTF behavior is observed in liquids, all of the pressure dependence can be described by the pressure

dependence of T_o. That clearly is not observed for polymers in the present work and thus sheds doubt on the assertion that the ionic conductivity in polymers is "liquid-like."

The isothermal studies can also be used to determine activation volumes directly via:

$$\Delta V^* = -kT \, d\ln\sigma/dP \qquad (5)$$

The zero pressure values are listed in Table III. As the values are calculated from pressure runs where curvature has been included, the updated values are somewhat less than the preliminary values reported previously.[18] However, they are still on the order of the values reported for ion containing PEO.[25] Further, the trend is the same in that the activation volume for perchlorate complexed material is larger than for thiocyanate complexed material. However, as reported previously,[18] ΔV^* for the triflate complexed material is smaller than for either thiocyanate or perchlorate complexed PPO. In addition, in the present work it is found that the iodide complexed material has a very large activation volume. As the iodide is the smallest ion, the results cannot be explained solely on the basis of the size of the anion.

Before suggesting an explanation, it is interesting to plot all of the activation volumes vs. $T-T_o$. Those results are shown in Fig. 4. The plot shows that an alternative view of the activation volume is that it is the approximately the same for all materials at a given temperature interval above T_o. Consequently, different activation volumes can merely be attributed to different T_o's. It is also noted that the activation

volume calculated from Eq. (5) decreases as temperature increases. This agrees with previous observations in PEO[25,26] and is expected as in general the activation volume scales with activation energy (slope of the conductivity plot) and the activation energy clearly decreases as temperature increases as is apparent from Fig. 2.

However, in either view, it is left to explain the trend with ion species. Clearly, only a limited sampling of ions has been examined. However, one possible explanation is suggested. Namely, the activation volume (and T_o or T_g) is smallest for ions for which the lithium transport number may be largest. Specifically, the data in the literature imply that for PEO complexed with lithium iodide and lithium perchlorate, the lithium transport number is about 0.3[27,28] whereas for PEO compexed with lithium thiocyanate and lithium triflate the lithium transport numbers are on the order of 0.5[29] and 0.7[28] respectively. Consequently, a combination of ion size and transport number may be responsible for the observed trends. For example, the small values of ΔV^* (and T_g or T_o) for the material complexed with the large triflate ion may be related to the comparatively large fraction of small, mobile lithium ions. Similarly, the large value of ΔV^* for the LiI complexed material may be related to the relatively small fraction of mobile lithium ions. Obviously, this suggestion is highly speculative in that the transport number data are for PEO and not PPO. However, it is interesting in that an explanation for the transport number differences is further suggested. Namely, thiocyanate and triflate have a permanent dipole moment while perchlorate and iodide do not. Consequently, because of this dipole moment, it may be that the former interact more strongly with the chains and thus contribute less to the electrical

conductivity. Obviously, ion size will also affect the magnitude of the transport numbers. Clearly, further work concerning these points is necessary.

It is noted that the curvature in the conductivity vs. pressure data such as shown in Fig. 3 and entries in Table III is opposite that reported for PEO.[25] It is likely that the different apparent curvature for PEO is due to electrode effects in that the early work on PEO was single frequency data and not the results of complex impedance analysis. The data for PEO are being redone and preliminary results indicate that the correct curvature is similar to that observed in the present work on PPO.

It will be of interest to determine both the compressibility and thermal expansion coefficient for these materials. In addition to allowing corrections of the conductance data, such data will make it possible to calculate the volume independent temperature variation and the temperature independent volume variation of the conductivity. Such experiments are currently underway.

Next, the data were analyzed in terms of the WLF equation:[30]

$$\log_{10} \frac{\sigma(T)}{\sigma(T_g)} = \frac{C_1(T-T_g)}{C_2+(T-T_g)} \qquad (6)$$

The resultant parameters are listed in Table I. The values of C_1 and/or C_2 are reasonably close to the "universal" values of 17.4 and 51.6.

Finally, for completeness, the data were analyzed via the VTF eq. in the form:

$$\sigma = A' \exp^{-[E'_a/(T-T'_o)]} \qquad (7)$$

which is analytically identical to the WLF equation with $T_o' = T_g - C_2$, $E_a' = 2.303C_1C_2$ and $\ln A' = 2.303C_1 + \ln\sigma(T_g)$. The results are also listed in Table II.

C. Electrical Relaxation

For comparison with the effect of pressure on the electrical conductivity, the effect of pressure on the α relaxation, that associated with the glass transition, was studied. As mentioned above, a preliminary report of single frequency data (the frequency, 1000 Hz was inadvertently omitted from the paper) at a variety of pressures has been given previously.[18] Typical variable frequency data are shown in Fig. 5. In each case, the peak position, ω_p, was obtained by best-fitting the imaginary part of the Havriliak-Negami function:[31]

$$C^* = \frac{D}{[1 + (i\omega\tau_o)^{(1-\alpha)}]^\beta} \qquad (8)$$

to the data where D, β, τ_o, and α are the fitting parameters. The vacuum results are shown in Fig. 6 where VTF or WLF behavior is once again obtained. The following VTF equation was best-fit to the data:

$$\omega_p = AT^{-1/2} \exp^{-[E_a/k(T-T_o)]} \qquad (9)$$

and the results are listed in Table II. It is seen that for three materials E_a is very close to the vacuum values obtained for the electrical conductivity for the complexed material. The exception is PPO_8:LiSCN, for

which, as described in Part II, the data are considered less reliable. In addition, by comparison with the DSC results listed in Table I, it is seen that T_o is once again observed to be about 40°C below T_g. Clearly, these results show a relation between the electrical conductivity and the α relaxation and hence between electrical conductivity and the glass transition.

For completeness, the analytically equivalent equations:

$$\log_{10} \frac{\omega_p(T)}{\omega_p(T_g)} = \frac{C_1(T-T_g)}{C_2+(T-T_g)} \qquad (10)$$

and

$$\omega_p = A' \exp^{-[E'_a/(T-T'_o)]} \qquad (11)$$

were also best-fit to the data and the results are listed in Tables I and II.

Next, the equation:

$$\log_{10}\omega_p = \log_{10}\omega_{p_o} + aP + bP^2 \qquad (12)$$

was best-fit to the isothermal electrical relaxation data. Typical data and best fit curve are shown in Fig. 7. The best-fit parameters along with the zero pressure activation volumes calculated from:

$$\Delta V^* = -kT \, d\ln\omega_p/dP \qquad (13)$$

are listed in Table III. For comparison, the activation volumes are plotted in Fig. 4. It is seen that to within the scatter in the data, on

the "reduced plot" they are the same as those for the electrical conductivity. This provides strong, albeit indirect evidence that electrical conductivity is controlled by the same mechanism as the α relaxation. Specifically, it provides evidence that ionic conductivity is controlled by the large scale segmental motions characteristic of the glass-rubber transition.

The idea that ionic conductivity in polymers is related to the α relaxation is not new, of course. For example, the concept is mentioned by Fuoss[32] as early as 1941. Further, many authors have suggested that the large ionic conductivity in PEO is associated with chain mobility.[1,33] However, it is to be emphasized that the above comments do not necessarily apply to the "transport mechanism." Specifically, in order for the results of the present work to imply that the electrical transport mechanism be due to large scale segmental motions, it is necessary that the number of mobile ions not change with temperature. That such is the case is not clear at the present time. In fact, it may be that all or part of the role of the large scale segmental motions is to control the degree of dissociation of the ions. Detailed microscopic experiments such as NMR will be useful toward separating out these effects.

IV. SUMMARY

In summary, then, the following results have been obtained:

(a) It has been found that both electrical conductivity in complexed PPO and the electrical relaxation associated with the glass transition in uncomplexed PPO exhibit the same pressure and temperature dependence. This represents evidence that ionic conductivity is controlled by the large

scale segmental motions characteristic of the glass-rubber transition.

(b) It has been shown that E_a cannot be considered a constant, independent of pressure, and thus the data are different from that for ionic conductivity in liquids.

(c) It has been found that T_o does not change much with pressure for materials with a high T_g or T_o i.e. materials for which large shifts in T_g or T_o have been caused by the presence of ions. This implies that T_g does not change much with pressure for those materials.

ACKNOWLEDGMENTS

The authors would like to thank Hercules, Inc. for supplying the Parel 58 elastomer. This work was supported in part by the Office of Naval Research. The authors would like to thank Dr. A. Tompa of NSWC, Indian Head for arranging for them to obtain the DSC Console.

REFERENCES

1. M. Armand, Solid State Ionics 9&10, 745 (1983).

2. P. M. Blonsky, D. F. Shriver, P. Austin, and H. R. Allcock, J. Am. Chem. Soc., 106, 6854 (1984).

3. S. G. Greenbaum, Solid State Ionics, 15, 259 (1985).

4. L. C. Hardy and D. F. Shriver, J. Am. Chem. Soc., 107, 3823 (1985).

5. D. W. Xia, D. Soltz, and J. Smid, Solid State Ionics, 221, 14 (1984).

6. K. Shigehara, N. Kobayashi, and E. Tsuchida, Solid State Ionics, 14, 85 (1984).

7. M. Watanabe, M. Rikukawa, K. Sanui, N. Ogata, Hisaaki Kato, T. Kobayashi, and Z. Ohtaki, Macromolecules, 17, 2902 (1984).

8. R. D. Armstrong and M. D. Clarke, Electrochimica Acta, 29, 1443 (1984).

9. C. K. Chiang, G. T. Davis, C. A. Harding, and T. Takahashi, Macromolecules, 18 825 (1985).

10. J. R. MacCallum, M. J. Smith, and C. A. Vincent, Solid State Ionics, 11, 307 (1984).

11. D. J. Bannister, G. R. Davies, I. M. Ward, and J. E. McIntyre, Polymer, 25, 1291 (1984); Polymer, 25, 1600 (1984).

12. A. Bouridah, F. Dalard, D. Deroo, H. Cheradame, J. F. LeNest, Solid State Ionics, 15, 233 (1985).

13. K. J. Adamic, S. G. Greenbaum, M. C. Wintersgill, and J. J. Fontanella, J. Appl. Phys., to be published.

14. M. B. Armand, J. M. Chabagno and M. J. Duclot, in Fast Ion Transport in Solids, J. N. Mundy and G. K. Shenoy, Eds., Pergamon Press, New York, 1979, p. 131.

REFERENCES

1. M. Armand, Solid State Ionics 9&10, 745 (1983).

2. P. M. Blonsky, D. F. Shriver, P. Austin, and H. R. Allcock, J. Am. Chem. Soc., 106, 6854 (1984).

3. S. G. Greenbaum, Solid State Ionics, 15, 259 (1985).

4. L. C. Hardy and D. F. Shriver, J. Am. Chem. Soc., 107, 3823 (1985).

5. D. W. Xia, D. Soltz, and J. Smid, Solid State Ionics, 221, 14 (1984).

6. K. Shigehara, N. Kobayashi, and E. Tsuchida, Solid State Ionics, 14, 85 (1984).

7. M. Watanabe, M. Rikukawa, K. Sanui, N. Ogata, Hisaaki Kato, T. Kobayashi, and Z. Ohtaki, Macromolecules, 17, 2902 (1984).

8. R. D. Armstrong and M. D. Clarke, Electrochimica Acta, 29, 1443 (1984).

9. C. K. Chiang, G. T. Davis, C. A. Harding, and T. Takahashi, Macromolecules, 18 825 (1985).

10. J. R. MacCallum, M. J. Smith, and C. A. Vincent, Solid State Ionics, 11, 307 (1984).

11. D. J. Bannister, G. R. Davies, I. M. Ward, and J. E. McIntyre, Polymer, 25, 1291 (1984); Polymer, 25, 1600 (1984).

12. A. Bouridah, F. Dalard, D. Deroo, H. Cheradame, J. F. LeNest, Solid State Ionics, 15, 233 (1985).

13. K. J. Adamic, S. G. Greenbaum, M. C. Wintersgill, and J. J. Fontanella, J. Appl. Phys., to be published.

14. M. B. Armand, J. M. Chabagno and M. J. Duclot, in Fast Ion Transport in Solids, J. N. Mundy and G. K. Shenoy, Eds., Pergamon Press, New York, 1979, p. 131.

15. M. Watanabe, K. Sanui, N. Ogata, T. Kobayashi, and Z. Ohtaki, J. Appl. Phys., 57, 123 (1985).

16. M. Watanabe, K. Sanui, N. Ogata, F. Inoue, T. Kobayashi, and Z. Ohtaki, Polym. J., 17, 549 (1985); Polym. J., 16, 711 (1984).

17. M. Watanabe, J. Ikeda, and I. Shinohara, Polym. J., 15, 65 (1983).

18. J. J. Fontanella, M. C. Wintersgill, J. P. Calame, M. K. Smith, and C. G. Andeen, Solid State Ionics, 18&19, 253 (1986).

19. H. Vogel, Physik Z., 22, 645 (1921); V.G. Tammann and W. Hesse, Z. Anorg. Allg. Chem., 156, 245 (1926); G.S. Fulcher, J. Am. Ceram. Soc., 8, 339 (1925).

20 C. A. Angell, Solid State Ionics, 9&10, 3 (1983).

21. B. L. Papke, M. A. Ratner, and D. F. Shriver, J. Electrochem. Soc. 129, 1434 (1982).

22. J. H. Gibbs and E.A. DiMarzio, J. Chem. Phys. 28 (1958) 373.

23. G. Adam and J.H. Gibbs, J. Chem. Phys. 43 (1965) 139.

24. C. A. Angell, L. J. Pollard, and W. Strauss, J. Solution Chemistry, 1, 517 (1972).

25. J. J. Fontanella, M. C. Wintersgill, J. P. Calame, F. P. Pursel, D. R. Figueroa, and C. G. Andeen, Solid State Ionics, 9&10, 1139 (1983).

26. A. V. Chadwick, J. H. Strange, and M. R. Worboys, Solid State Ionics 9&10, 1155 (1983).

27. J. E. Weston and B. C. H. Steele, Solid State Ionics 7, 75 (1982); 81 (1982).

28. A. Bouridah, F. Dalard, D. Deroo, and M. B. Armand, Solid State Ionics, 18&19, 287 (1986).

29. P. R. Sorensen and T. Jacobsen, Electrochimica Acta, 27, 1671 (1982).

30. M. L. Williams, R. F. Landel, and J. D. Ferry, J. Am. Chem. Soc., 77, 3701 (1955).

31. S. Havriliak and S. Negami, J. Polymer Science, C14, 99 (1966).

32. R. M. Fuoss, J. Am. Chem. Soc., 63, 369,378 (1941).

33. R. E. Barker, Jr., Pure & Appl. Chem., 46, 157 (1976).

TABLE I. DSC results and best fit WLF parameters.

		T_g(K)	C_1	C_2(K)	$\log_{10}\sigma(T_g)(\Omega\text{-cm})^{-1}$ [$\log_{10}\omega_p(T_g)(s^{-1})$]	RMS Deviation
Electrical Relaxation (α)						
Uncomplexed PPO	Onset	208	12.6	35.3	[0.089]	0.0038
	Central	211	11.6	38.3	[1.076]	0.0038
	End	215	10.5	42.3	[2.174]	0.0038
Electrical Conductivity						
$PPO_8LiCF_3SO_3$	Onset[a]	238	18.7	22.0	-21.0	0.0146
	Central	248	12.9	32.0	-15.2	0.0146
	End	258	9.8	42.0	-12.1	0.0146
PPO_8LiClO_4	Onset[a]	263	14.8	26.4	-16.2	0.0111
	Central	281	8.8	44.4	-10.2	0.0111
	End	299	6.2	62.4	-7.7	0.0111
PPO_8LiI	Onset	268	18.9	21.9	-19.7	0.0233
	Central	283	11.2	36.9	-12.0	0.0233
	End	298	7.96	51.9	-8.76	0.0233
PPO_8LiSCN	Onset[a]	245	15.2	39.9	-16.1	0.0087
	Central	266	9.94	60.9	-10.9	0.0087
	End	285	7.58	79.9	-8.53	0.0087

a. Reference 18.

TABLE II. Best fit VTF parameters.

	RMS Deviation	$\log_{10}A$ $(\Omega\text{-cm})^{-1}\text{-}\sqrt{K}$ $[s^{-1}\text{-}\sqrt{K}]$	E_a(eV)	T_o(K)	RMS Deviation	$\log_{10}A'$ $(\Omega\text{-cm})^{-1}$ $[s^{-1}]$	E'_a(eV)	T'_o(K)
Uncomplexed PPO, electrical relaxation (α)								
Vacuum	0.0038	[13.95]	0.089	172.5	0.0038	[12.68]	0.088	172.7
$PPO_8LiCF_3SO_3$, electrical conductivity								
Vacuum[a]	0.0143	-0.94	0.086	214.0	0.0146	-2.34	0.082	216.0
0.1 GPa[a]	0.0054	-1.02	0.098	216.2	0.0055	-2.42	0.093	217.9
0.1 GPa[b]	0.0145	-1.06	0.086	226.2	0.0148	-2.45	0.082	227.6
0.2 GPa[a]	0.0142	-0.73	0.104	232.9	0.0143	-2.11	0.101	233.9
0.2 GPa[b]	0.0242	-1.03	0.092	233.6	0.0244	-2.41	0.089	234.6
PPO_8LiCLO_4, electrical conductivity								
Vacuum[a]	0.0110	-0.04	0.082	234.9	0.0111	-1.44	0.077	236.6
0.1 GPa[b]	0.0170	+1.11	0.094	236.4	0.0172	-0.26	0.091	237.4
0.1 GPa[b]	0.0435	+0.44	0.112	230.3	0.0436	-0.94	0.108	231.3
0.2 GPa[b]	0.0196	+1.03	0.103	242.6	0.0197	-0.34	0.100	243.3
0.2 GPa[b]	0.0692	+0.63	0.128	234.2	0.0692	-0.75	0.125	234.9
PPO_8LiI, electrical conductivity								
Vacuum	0.0226	+0.56	0.085	245.3	0.0233	-0.80	0.082	246.1
0.1 GPa[b]	0.0113	+0.97	0.114	240.3	0.0113	-0.40	0.111	241.0
0.1 GPa[b]	0.0304	+0.75	0.104	244.4	0.0303	-0.62	0.101	245.1
0.2 GPa[b]	0.0181	+0.72	0.127	241.1	0.0182	-0.66	0.124	241.8
0.2 GPa[b]	0.0822	+1.02	0.126	244.2	0.0820	-0.35	0.123	244.8
PPO_8LiSCN, electrical conductivity								
Vacuum[a]	0.0086	+0.047	0.126	203.2	0.0087	-0.95	0.120	205.1

a. Reference 18.
b. Calculated from isothermal data runs using the vacuum isobaric data as a reference.

TABLE III. Best fit parameters (Eqs. 4 and 12) and activation volumes for isothermal data.

	T(K)	RMS Deviation	$\log_{10}\sigma(\Omega\text{-cm})^{-1}$ [$\log_{10}\omega_{p_o}(s^{-1})$]	a(GPa)$^{-1}$	b(GPa)$^{-2}$	ΔV^* (cm^3/mol)
Electrical Relaxation (α)						
Uncomplexed PPO	237.1	0.0055	[6.176]	-17.94	-26.5	81.4
	243.6	0.0071	[6.550]	-17.11	-21.3	79.8
	253.1	0.0079	[7.121]	-12.51	-18.4	60.7
	273.1	0.0063	[8.186]	-8.88	-8.49	46.4
Electrical Conductivity						
$PPO_8LiCF_3SO_3$	303.4	0.0181	-7.055	-7.72	-8.61	44.8
	320.8	0.0069	-6.272	-5.74	-5.34	35.3
	333.2	0.0138	-5.856	-4.95	-3.72	31.6
	349.1	0.0307	-5.436	-3.69	-3.16	24.7
	357.8	0.0241	-5.244	-3.51	-2.16	24.0
	370.4	0.0064	-5.008	-3.49	-1.11	24.7
PPO_8LiClO_4	303.0	0.0051	-7.303	-11.32	-11.80	65.7
	309.8	0.0172	-6.753	-10.60	-6.58	62.9
	323.1	0.0076	-5.938	-8.95	-5.25	55.4
	332.9	0.0139	-5.480	-8.15	-1.99	52.0
	343.1	0.0182	-5.093	-7.72	-0.37	50.7
	354.0	0.0822	-4.753	-5.03	-3.53	34.1
	369.4	0.0397	-4.370	-5.60	-0.42	39.6
PPO_8LiI	302.9	0.0070	-8.078	-12.20	-13.52	70.8
	309.9	0.0136	-7.281	-11.05	-9.46	65.5
	332.9	0.0026	-5.562	-7.61	-5.13	48.5
	343.1	0.0063	-5.061	-7.41	-7.07	48.7
	363.1	0.0193	-4.334	-5.70	-3.14	39.6
	369.4	0.0285	-4.156	-5.31	-1.76	37.5
PPO_8LiSCN[a]	323.1	0.0385	-6.081	-4.34	-4.33	26.8
	343.1	0.0059	-5.337	-3.62	-2.43	23.8
	363.1	0.0068	-4.782	-3.66	-1.01	25.4

a. Reference 18.

FIGURE CAPTIONS

Figure 1. DSC thermograms for (a) Uncomplexed PPO, (b) PPO_8LiI after quench from 200°C, (c) As-prepared PPO_8LiI.

Figure 2. Data and best-fit VTF curve (Eq. (3)) curves for the temperature dependence of the ionic conductivity for PPO_8LiI (a) in vacuum, (b) at 0.1 GPa, and (c) at 0.2 GPa.

Figure 3. Data and best-fit quadratic (Eq. (4)) for the pressure dependence of the ionic conductivity for PPO_8LiClO_4 at 369.4K.

Figure 4. Activation volumes vs. reduced temperature for (a) x-the electrical relaxation time for the α relaxation and the electrical conductivity for (b) ◇-$PPO_8LiCF_3SO_3$, (c) □-PPO_8LiClO_4, (d) Δ-PPO_8LiI, and (e) *-PPO_8LiSCN.

Figure 5. Data and best-fit Havriliak-Negami curves (Eq. (8)) for dielectric loss vs. frequency for the α relaxation at (a) 0.16 GPa, (b) 0.12 GPa, and (c) 0.08 GPa.

Figure 6. Data and best-fit VTF curve (Eq. (9)) for the ~~relaxation time~~ peak position for the α relaxation for uncomplexed PPO.

Figure 7. Data and best-fit quadratic (Eq. (12)) for the ~~relaxation time~~ peak position for the α relaxation at 237.1K.

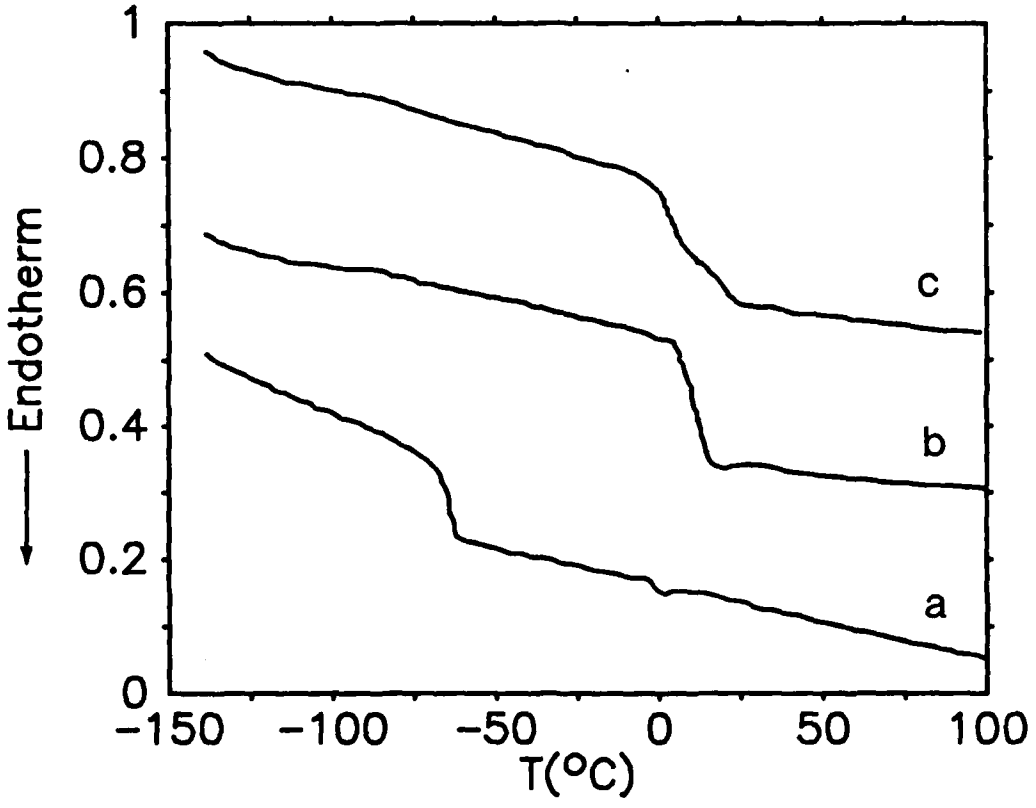

Fig. 1 Fontanella et al.

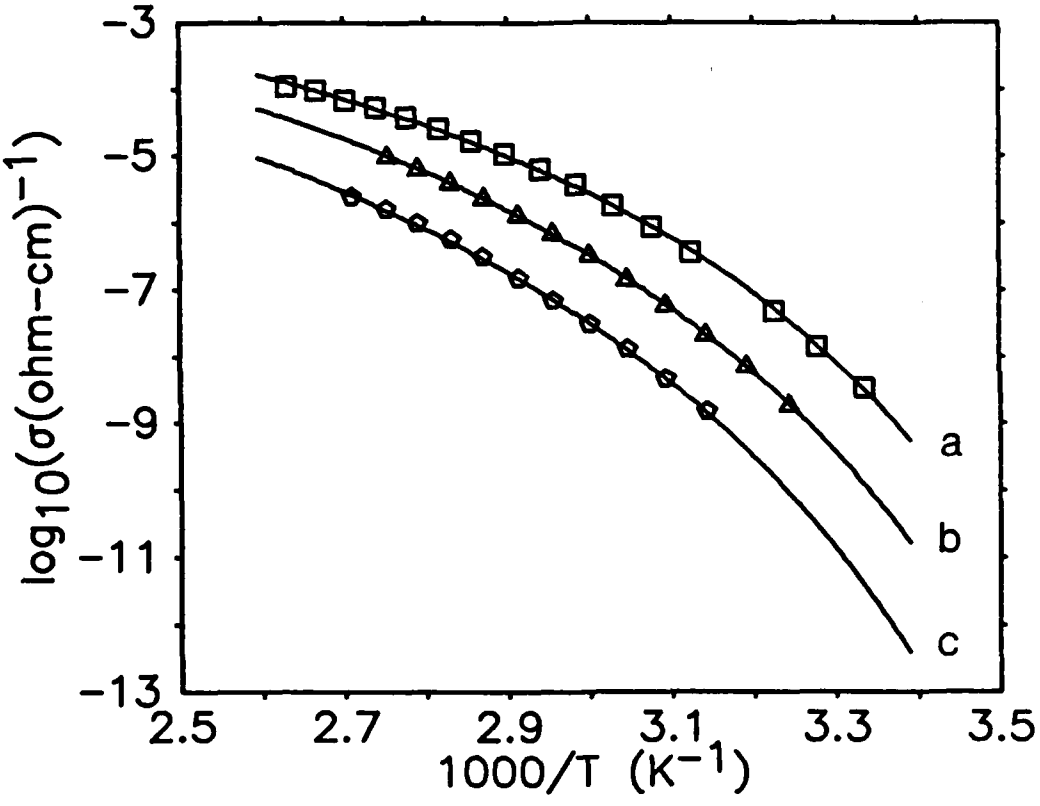

Fig. 2 Fontanella et al.

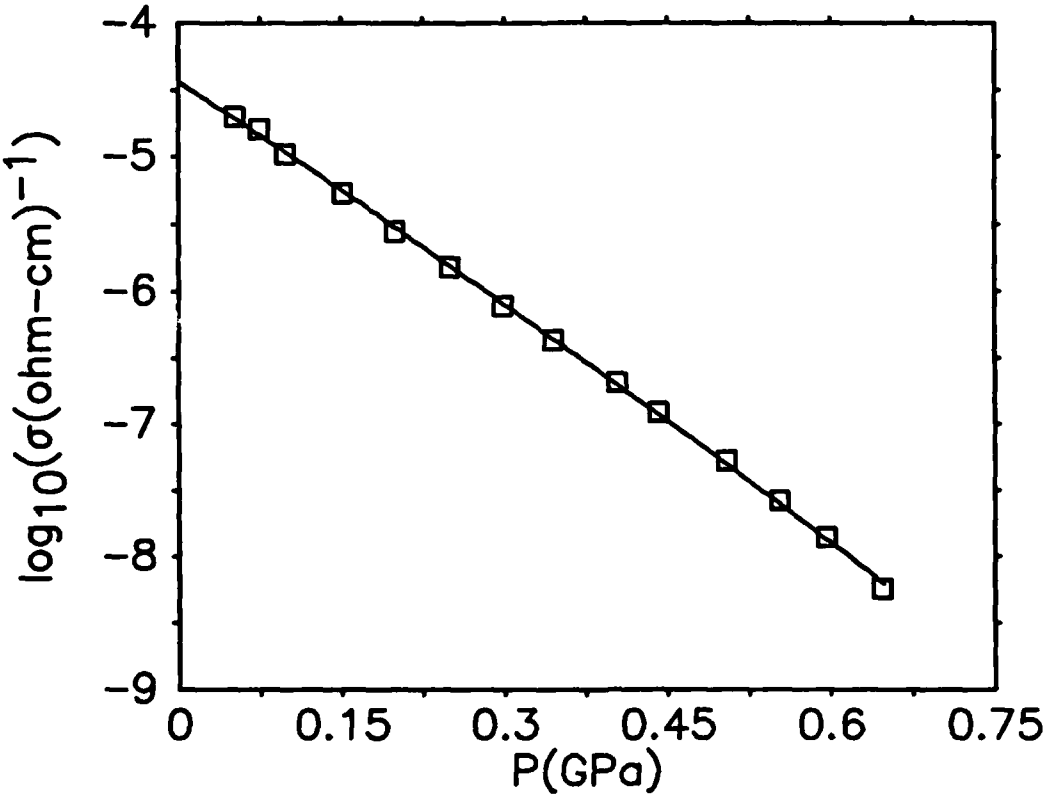

Fig 3 Fontanella et al

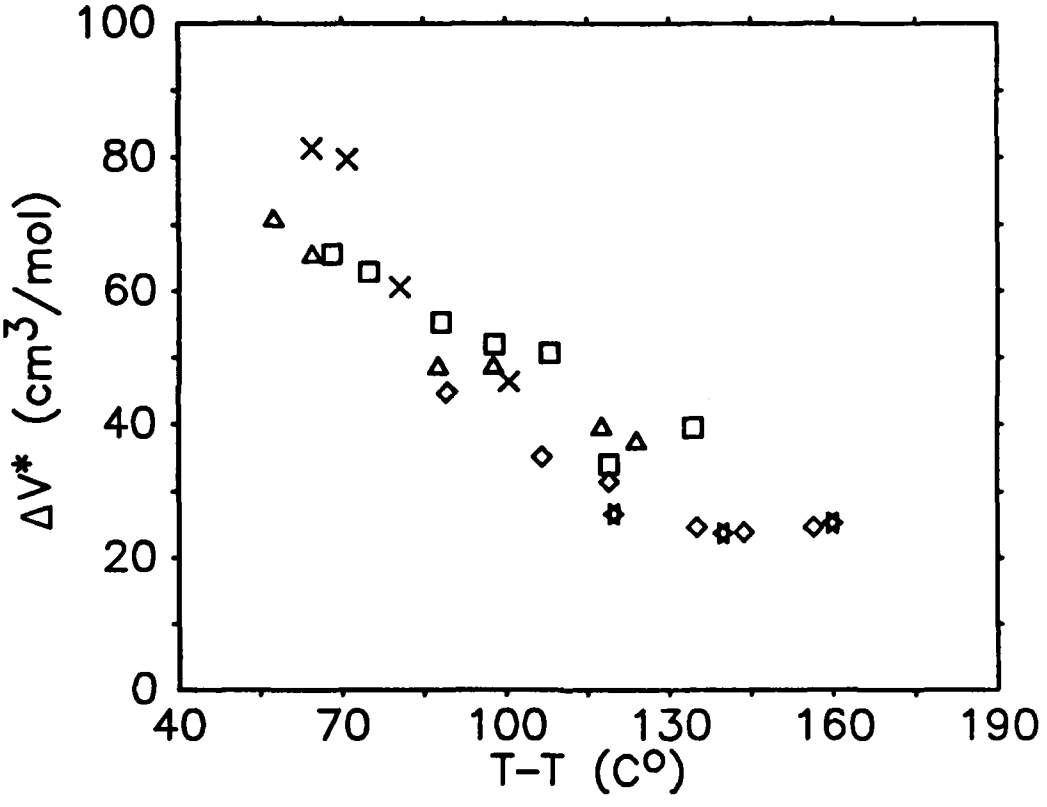

Fig. 4 Fontanella et al

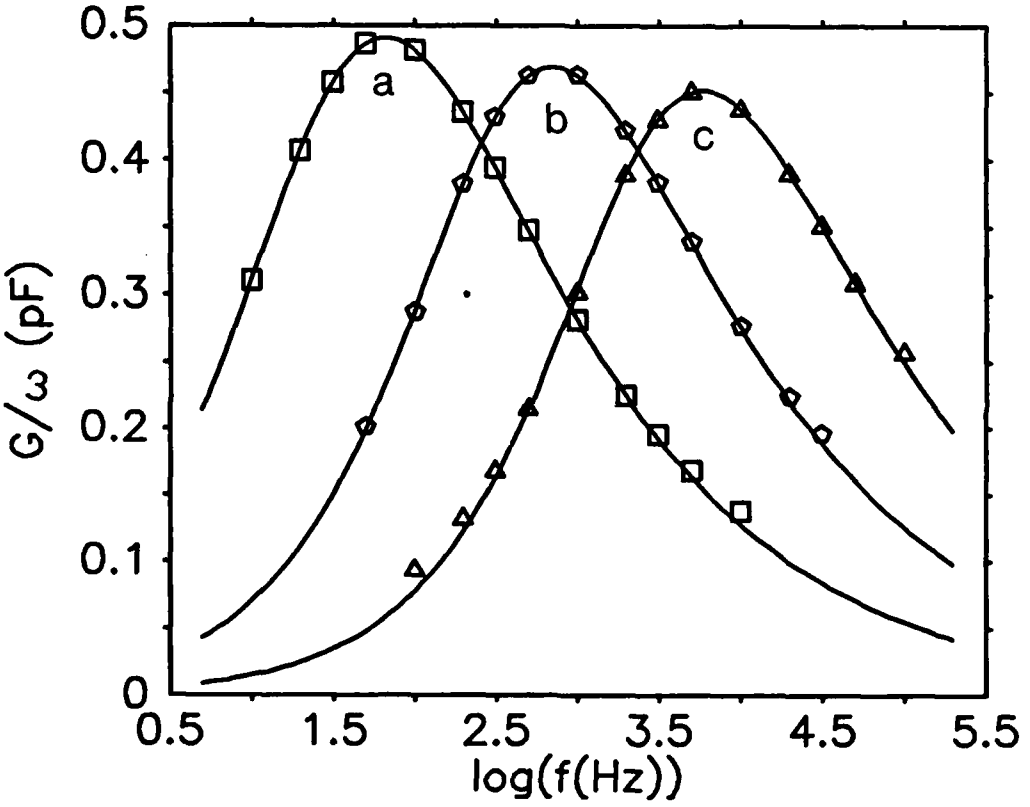

Fig 5 Fontanella et al.

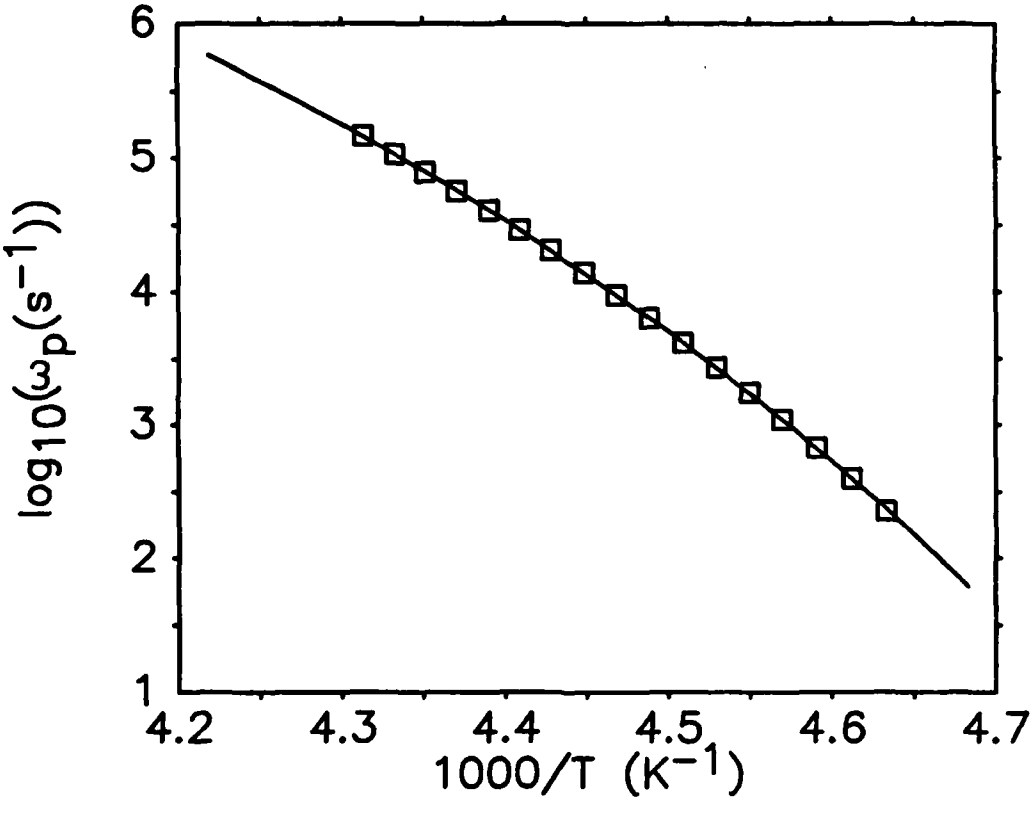

Fig 6 Fontanella et al.

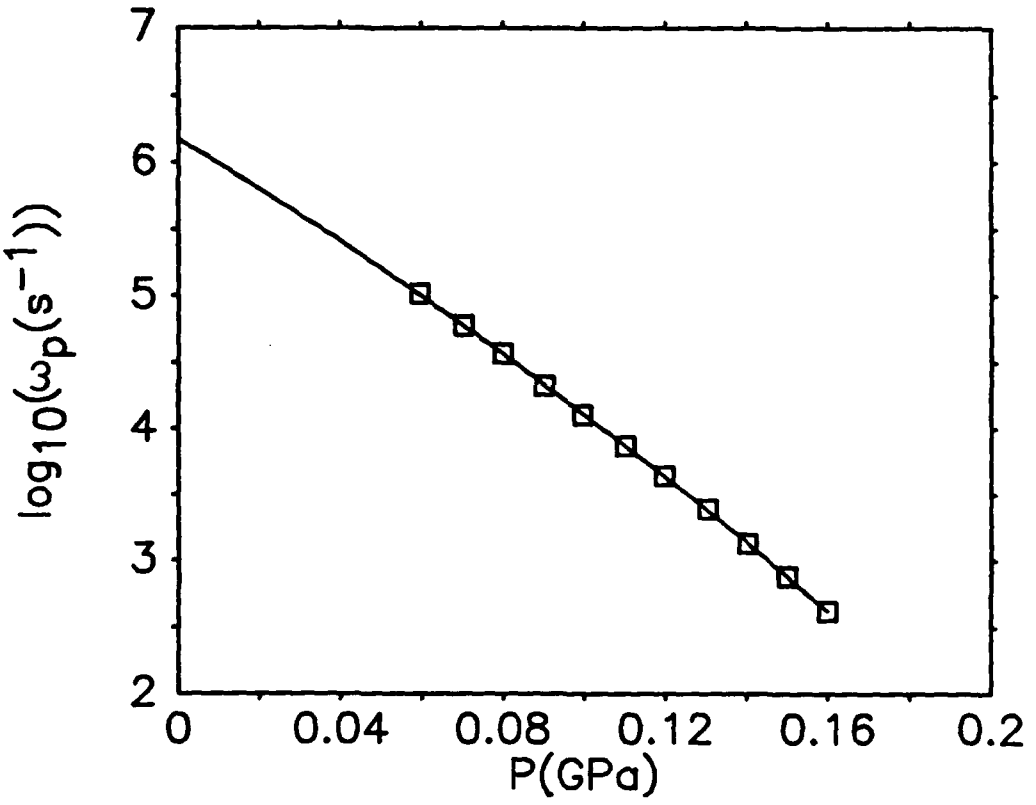

Fig 2 Fontanella et al.

OL/413/83/01
GEN/413-2

TECHNICAL REPORT DISTRIBUTION LIST, GEN

	No. Copies
Office of Naval Research Attn: Code 413 800 N. Quincy Street Arlington, Virginia 22217	2
Dr. Bernard Douda Naval Weapons Support Center Code 5042 Crane, Indiana 47522	1
Commander, Naval Air Systems Command Attn: Code 310C (H. Rosenwasser) Washington, D.C. 20360	1
Naval Civil Engineering Laboratory Attn: Dr. R. W. Drisko Port Hueneme, California 93401	1
Defense Technical Information Center Building 5, Cameron Station Alexandria, Virginia 22314	12
DTNSRDC Attn: Dr. G. Bosmajian Applied Chemistry Division Annapolis, Maryland 21401	1
Dr. William Tolles Superintendent Chemistry Division, Code 6100 Naval Research Laboratory Washington, D.C. 20375	1
Dr. David Young Code 334 NORDA NSTL, Mississippi 39529	1
Naval Weapons Center Attn: Dr. Ron Atkins Chemistry Division China Lake, California 93555	1
Scientific Advisor Commandant of the Marine Corps Code RD-1 Washington, D.C. 20380	1
U.S. Army Research Office Attn: CRD-AA-IP P.O. Box 12211 Research Triangle Park, NC 27709	1
Mr. John Boyle Materials Branch Naval Ship Engineering Center Philadelphia, Pennsylvania 19112	1
Naval Ocean Systems Center Attn: Dr. S. Yamamoto Marine Sciences Division San Diego, California 91232	1

DL/413/83/01
359/413-2

ABSTRACTS DISTRIBUTION LIST, 359/627

Dr. Paul Delahay
Department of Chemistry
New York University
New York, New York 10003

Dr. P. J. Hendra
Department of Chemistry
University of Southampton
Southampton SO9 5NH
United Kingdom

Dr. J. Driscoll
Lockheed Palo Alto Research
Laboratory
3251 Hanover Street
Palo Alto, California 94304

Dr. D. N. Bennion
Department of Chemical Engineering
Brigham Young University
Provo, Utah 84602

Dr. R. A. Marcus
Department of Chemistry
California Institute of Technology
Pasadena, California 91125

Dr. J. J. Auborn
Bell Laboratories
Murray Hill, New Jersey 07974

Dr. Joseph Singer, Code 302-1
NASA-Lewis
21000 Brookpark Road
Cleveland, Ohio 44135

Dr. P. P. Schmidt
Department of Chemistry
Oakland University
Rochester, Michigan 48063

Dr. Manfred Breiter
Institut fur Technische Elektrochemie
Technischen Universitat Wien
9 Getreidemarkt, 1160 Wien
AUSTRIA

Dr. E. Yeager
Department of Chemistry
Case Western Reserve University
Cleveland, Ohio 44106

Dr. C. E. Mueller
The Electrochemistry Branch
Naval Surface Weapons Center
White Oak Laboratory
Silver Spring, Maryland 20910

Dr. Sam Perone
Chemistry & Materials
Science Department
Lawrence Livermore National Laboratory
Livermore, California 94550

Dr. Royce W. Murray
Department of Chemistry
University of North Carolina
Chapel Hill, North Carolina 27514

Dr. B. Brummer
EIC Incorporated
111 Downey Street
Norwood, Massachusetts 02062

Dr. Adam Heller
Bell Laboratories
Murray Hill, New Jersey 07974

Dr. A. B. Ellis
Chemistry Department
University of Wisconsin
Madison, Wisconsin 53706

Library
Duracell, Inc.
Burlington, Massachusetts 01803
wrong address

Electrochimica Corporation
20 Kelly Court
Menlo Park, California 94025-1418

DL/413/83/01
359/413-2

ABSTRACTS DISTRIBUTION LIST, 359/627

Dr. John Owen
Department of Chemistry and
Applied Chemistry
University of Salford
Salford M5 4WT ENGLAND

Dr. Boone Owens
Department of Chemical Engineering
and Materials Science
University of Minnesota
Minneapolis, Minnesota 55455

Dr. J. O. Thomas
University of Uppsala
Institute of Chemistry
Box 531
S-751 21 Uppsala, Sweden

Dr. O. Stafsudd
Department of Electrical Engineering
University of California
Los Angeles, California 90024

Dr. S. G. Greenbaum
Department of Physics
Hunter College of CUNY
New York, New York 10021

Dr. Menahem Anderman
W.R. Grace & Co.
Columbia, Maryland 20144

DL/413/83/01
359/413-2

ABSTRACTS DISTRIBUTION LIST, 359/627

Dr. Robert Somoano
Jet Propulsion Laboratory
California Institute of Technology
Pasadena, California 91103

Dr. Johann A. Joebstl
USA Mobility Equipment R&D Command
DRDME-EC
Fort Belvoir, Virginia 22060

Dr. Judith H. Ambrus
NASA Headquarters
M.S. RTS-6
Washington, D.C. 20546

Dr. Albert R. Landgrebe
U.S. Department of Energy
M.S. 6B025 Forrestal Building
Washington, D.C. 20595

Dr. J. J. Brophy
Department of Physics
University of Utah
Salt Lake City, Utah 84112

Dr. Charles Martin
Department of Chemistry
Texas A&M University
College Station, Texas 77843

Dr. H. Tachikawa
Department of Chemistry
Jackson State University
Jackson, Mississippi 39217

Dr. Theodore Beck
Electrochemical Technology Corp.
3935 Leary Way N.W.
Seattle, Washington 98107

Dr. Farrell Lytle
Boeing Engineering and
Construction Engineers
P.O. Box 3707
Seattle, Washington 98124

Dr. Robert Gotscholl
U.S. Department of Energy
MS G-226
Washington, D.C. 20545

Dr. Edward Fletcher
Department of Mechanical Engineering
University of Minnesota
Minneapolis, Minnesota 55455

Dr. John Fontanella
Department of Physics
U.S. Naval Academy
Annapolis, Maryland 21402

Dr. Martha Greenblatt
Department of Chemistry
Rutgers University
New Brunswick, New Jersey 08903

Dr. John Wasson
Syntheco, Inc.
Rte 6 - Industrial Pike Road
Gastonia, North Carolina 28052

Dr. Walter Roth
Department of Physics
State University of New York
Albany, New York 12222

Dr. Anthony Sammells
Eltron Research Inc.
4260 Westbrook Drive, Suite 111
Aurora, Illinois 60505

Dr. C. A. Angell
Department of Chemistry
Purdue University
West Lafayette, Indiana 47907

Dr. Thomas Davis
Polymer Science and Standards
Division
National Bureau of Standards
Washington, D.C. 20234

Ms. Wendy Parkhurst
Naval Surface Weapons Center R-33
R-33
Silver Spring, Maryland 20910

DL/413/83/01
359/413-2

ABSTRACTS DISTRIBUTION LIST, 359/627

Dr. Hector D. Abruna
Department of Chemistry
Cornell University
Ithaca, New York 14853

Dr. A. B. P. Lever
Chemistry Department
York University
Downsview, Ontario M3J1P3

Dr. Stanislaw Szpak
Naval Ocean Systems Center
Code 633, Bayside
San Diego, California 95152

Dr. Gregory Farrington
Department of Materials Science
and Engineering
University of Pennsylvania
Philadelphia, Pennsylvania 19104

M. L. Robertson
Manager, Electrochemical
and Power Sources Division
Naval Weapons Support Center
Crane, Indiana 47522

Dr. T. Marks
Department of Chemistry
Northwestern University
Evanston, Illinois 60201

Dr. Micha Tomkiewicz
Department of Physics
Brooklyn College
Brooklyn, New York 11210

Dr. Lesser Blum
Department of Physics
University of Puerto Rico
Rio Piedras, Puerto Rico 00931

Dr. Joseph Gordon, II
IBM Corporation
5600 Cottle Road
San Jose, California 95193

Dr. Nathan Lewis
Department of Chemistry
Stanford University
Stanford, California 94305

Dr. D. H. Whitmore
Department of Materials Science
Northwestern University
Evanston, Illinois 60201

Dr. Alan Bewick
Department of Chemistry
The University of Southampton
Southampton, SO9 5NH ENGLAND

Dr. E. Anderson
NAVSEA-56Z33 NC #4
2541 Jefferson Davis Highway
Arlington, Virginia 20362

Dr. Bruce Dunn
Department of Engineering &
Applied Science
University of California
Los Angeles, California 90024

Dr. Elton Cairns
Energy & Environment Division
Lawrence Berkeley Laboratory
University of California
Berkeley, California 94720

Dr. Richard Pollard
Department of Chemical Engineering
University of Houston
Houston, Texas 77004

Dr. M. Philpott
IBM Corporation
5600 Cottle Road
San Jose, California 95193

Dr. Donald Sandstrom
Boeing Aerospace Co.
P.O. Box 3999
Seattle, Washington 98124

Dr. Carl Kannewurf
Department of Electrical Engineering
and Computer Science
Northwestern University
Evanston, Illinois 60201

Dr. Joel Harris
Department of Chemistry
University of Utah
Salt Lake City, Utah 84112

ABSTRACTS DISTRIBUTION LIST, 359/627

Dr. M. Wrighton
Chemistry Department
Massachusetts Institute
of Technology
Cambridge, Massachusetts 02139

Dr. B. Stanley Pons
Department of Chemistry
University of Utah
Salt Lake City, Utah 84112

Donald E. Mains
Naval Weapons Support Center
Electrochemical Power Sources Division
Crane, Indiana 47522

S. Ruby
DOE (STOR)
Room 5E036 Forrestal Bldg., CE-14
Washington, D.C. 20595

Dr. A. J. Bard
Department of Chemistry
University of Texas
Austin, Texas 78712

Dr. Janet Osteryoung
Department of Chemistry
State University of New York
Buffalo, New York 14214

Dr. Donald W. Ernst
Naval Surface Weapons Center
Code R-33
White Oak Laboratory
Silver Spring, Maryland 20910

Mr. James R. Moden
Naval Underwater Systems Center
Code 3632
Newport, Rhode Island 02840

Dr. Bernard Spielvogel
U.S. Army Research Office
P.O. Box 12211
Research Triangle Park, NC 27709

Dr. Aaron Fletcher
Naval Weapons Center
Code 3852
China Lake, California 93555

Dr. M. M. Nicholson
Electronics Research Center
Rockwell International
3370 Miraloma Avenue
Anaheim, California

Dr. Michael J. Weaver
Department of Chemistry
Purdue University
West Lafayette, Indiana 47907

Dr. R. David Rauh
EIC Laboratories, Inc.
111 Downey Street
Norwood, Massachusetts 02062

Dr. Aaron Wold
Department of Chemistry
Brown University
Providence, Rhode Island 02192

Dr. Martin Fleischmann
Department of Chemistry
University of Southampton
Southampton SO9 5NH ENGLAND

Dr. R. A. Osteryoung
Department of Chemistry
State University of New York
Buffalo, New York 14214

Dr. John Wilkes
Air Force Office of Scientific
Research
Bolling AFB
Washington, D.C. 20332

Dr. R. Nowak
Naval Research Laboratory
Code 6171
Washington, D.C. 20375

Dr. D. F. Shriver
Department of Chemistry
Northwestern University
Evanston, Illinois 60201

END

DTIC

8-86